ChemPubSoc Europe

DOI: 10.1002/slct.201900615

Chemistry SELECT Communications

Catalysis

A Non-Pt Electronically Coupled Semiconductor Heterojunction for Enhanced Oxygen Reduction Electrocatalytic Property

Fan Li[+],[a] Yong Qin[+],[a] Aleksei Chalgin[+],[a] Xin Gu,[a] Wenlong Chen,[a] Yanling Ma,[a] Qian Xiang,[a] Yi Wu,[a] Fenglei Shi,[a] Yuan Zong,[a] Peng Tao,[a] Chengyi Song,[a] Wen Shang,[a] Tao Deng,[a, b] Hong Zhu,*[a, c, d] and Jianbo Wu*[a, b, d]

Hybrid faceted-Ag_3PO_4/cube-Cu_2O composite materials have been fabricated and employed as oxygen reduction electrocatalysts for proton exchange membrane fuel cells (PEMFCs). The charge separation effect via the formation of PN junction has been demonstrated to boost the electrocatalysis toward oxygen reduction reaction. The as-prepared rhombic dodecahedron-Ag_3PO_4/cube-Cu_2O/C hybrid catalyst shows a mass-specific activity of 109.80 mA/mg_{Ag}, which is about 6.4 times that of pure rhombic dodecahedron-Ag_3PO_4/C catalyst (17.20 mA/mg_{Ag}). The density functional theory (DFT) calculation based on the density of states (DOS) further proved the optimal tunable effect, which is in pace with demonstration of electron transfer direction revealed by X-ray photoelectron spectroscopy (XPS) analysis. Our work establishes a theoretical and practical basis for the rational design of newly non-Pt hybrid catalysts, moreover, advances the future efficient application of PEMFCs.

Main Text

Developing cost-effective proton-exchange membrane fuel cells (PEMFCs) plays a key role for a wide variety of clean energy applications.[1–3] The sluggish kinetics of oxygen reduction reaction (ORR) is still one of the most limiting factors.[1,4,5] Recently, the element distribution, composition and shape control of platinum-based electrocatalyst have been widely studied to reduce platinum usage and improve ORR activity.[6–13] It has been reported that the cost of Pt catalyst is about 50% in the whole fuel cell stack,[14] which limits its commercial application. Considering that Pt is scarcely available at high price, low storage and poor durability,[15] many researchers devote themselves to exploring non-Pt ORR catalysts, such as non-Pt metals (Pd,[16,17] Ag,[18] Fe,[19] etc.), metal oxide,[20] perovskite,[21] etc.

In our previous work, we presented good electrochemical performance of faceted Ag_3PO_4 towards ORR in alkaline solution according to the design principle of morphology engineering.[22] The charge separation of heterojunction photocatalyst between the Ag_3PO_4 and another semiconductor including $BiVO_4$,[23] AgBr,[24] Cu_2O,[25] TiO_2,[26] etc, has been widely explored to improve the photochemical activity and stability. Due to the suitable bandgap position and safety, the novel Ag_3PO_4 and Cu_2O composites have attracted much attention and been theoretically investigated for their outstanding electronic and photocatalytic properties. Presently, few researchers studied the ORR performance of the heterojunction between Ag_3PO_4 and another semiconductor on electrocatalysts viewed from the point of electronic modification effect.

In this paper, we build a PN junction cross the Ag_3PO_4/Cu_2O hybrid catalyst to manipulate the electron distribution through the interfacial engineering between Ag_3PO_4 and the Cu_2O. Both the experimental results and theoretical calculation show the strong synergistic electronic interactions between Ag_3PO_4 and Cu_2O semiconductors. The hybrid catalysts present better ORR performance than the pure Ag_3PO_4 catalyst contributed by the flow of electrons from Ag_3PO_4 to Cu_2O. This demonstration plays an important role in the design of hybrid catalysts and has great potential to design alternative non-Pt catalysts as well.

We have successfully synthesized tetrahedron-, rhombic dodecahedron- and cube-Ag_3PO_4 with smooth surfaces and sharp corners, which possess corresponding {111}, {110} and {100} facets (Figure S1a-c). At the same time, the regular cube-Cu_2O crystals (Figure S1d) were synthesized by the previous report.[27] Three types of Ag_3PO_4 with different facets were mixed with Cu_2O cubes in different mass ratio, respectively. After selecting the compound whose proportion of Ag_3PO_4 and

[a] Dr. F. Li,[+] Y. Qin,[+] Dr. A. Chalgin,[+] Dr. X. Gu, Dr. W. Chen, Dr. Y. Ma, Dr. Q. Xiang, Y. Wu, Dr. F. Shi, Y. Zong, Prof. P. Tao, Prof. C. Song, Prof. W. Shang, Prof. T. Deng, Prof. H. Zhu, Prof. J. Wu
State Key Laboratory of Metal Matrix Composites, School of Materials Science and Engineering, Shanghai Jiao Tong University, 800 Dongchuan Road, Shanghai 200240 (P. R. China)
E-mail: hong.zhu@sjtu.edu.cn
jianbowu@sjtu.edu.cn
[b] Prof. T. Deng, Prof. J. Wu
Center of Hydrogen Science, Shanghai Jiao Tong University
[c] Prof. H. Zhu
University of Michigan-Shanghai Jiao Tong University Joint Institute, Shanghai Jiao Tong University
[d] Prof. H. Zhu, Prof. J. Wu
Materials Genome Initiative Center, Shanghai Jiao Tong University
[+] The authors Fan Li, Yong Qin and Aleksei Chalgin, contributed equally to this article.

Supporting information for this article is available on the WWW under https://doi.org/10.1002/slct.201900615

© 2019 Wiley-VCH Verlag GmbH & Co. KGaA, Weinheim

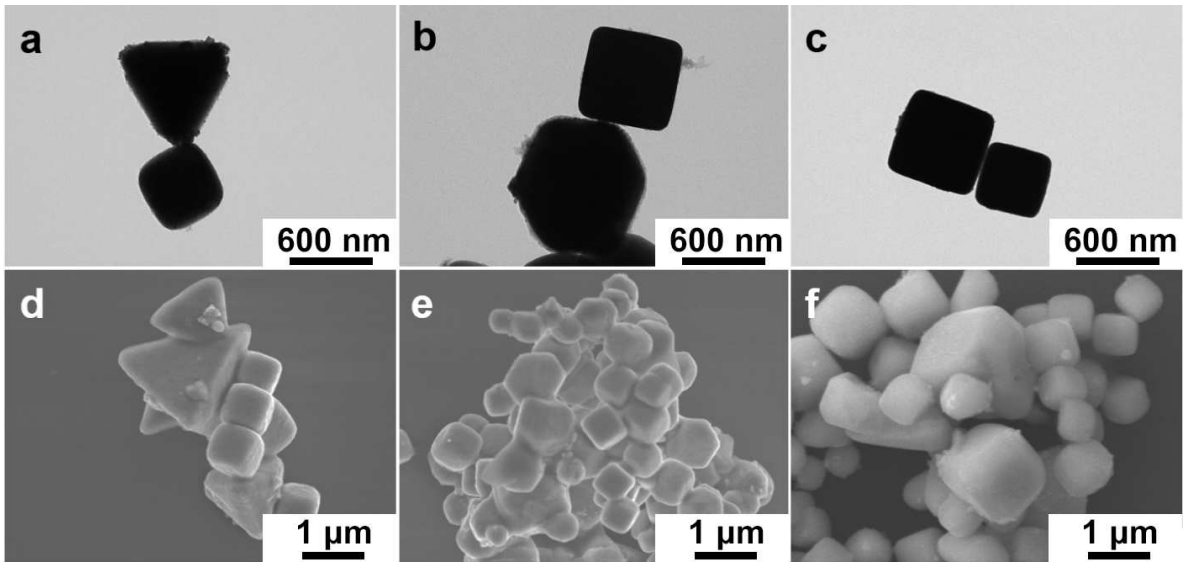

Figure 1. TEM micrograph of Ag_3PO_4 and Cu_2O hybrid catalysts. (a) tetrahedron-Ag_3PO_4 and cube-Cu_2O crystal, (b) rhombic dodecahedron-Ag_3PO_4 and cube-Cu_2O crystal, (c) cube-Ag_3PO_4 and cube-Cu_2O crystal. SEM micrograph of Ag_3PO_4 and Cu_2O hybrid catalysts: (d) tetrahedron-Ag_3PO_4 and cube-Cu_2O crystal, (e) rhombic dodecahedron-Ag_3PO_4 and cube-Cu_2O crystal, (f) cube-Ag_3PO_4 and cube-Cu_2O crystal.

Cu_2O is 1 to 0.125 for the SEM and TEM characterizations, we observed that the as-prepared cube-Cu_2O crystals were coupled closely to three types Ag_3PO_4 with {111}, {110} and {100} facets, respectively(Figure 1a-c). Their entirely well-distributed mixing was confirmed by the corresponding SEM images (Figure 1d-f). All the X-ray diffraction (XRD) patterns (Figure S2) indicated that the mixture is composed of Ag_3PO_4 and Cu_2O, which agrees well with the TEM observation.

The ORR performances of the three Ag_3PO_4/Cu_2O composites in different proportions were compared to the corresponding pure Ag_3PO_4. The ORR polarization curves (Figure S3a-c) show that there are shifts of both onset potential and half-wave potential for these three hybrid Ag_3PO_4/Cu_2O composites in different proportions compared with the corresponding pure faceted Ag_3PO_4 catalyst, which indicates the improved ORR performance after the mixing of Ag_3PO_4 particles with Cu_2O crystals. The enhancement of mass-specific activity in the change of hybrid proportions is summarized in Figure S3d-f and Table S1-3. The optimal mass ratio corresponding to the highest ORR performance of all the hybrid Ag_3PO_4 and Cu_2O system is 1: 0.125 (Figure S3d-f) and the ORR polarization curves of each composite with optimal mass ratio are shown in Figure 2a-c, respectively. The corresponding optimal mass activity of tetrahedron-, rhombic dodecahedron- and cube-Ag_3PO_4/cube-Cu_2O/C catalysts is 99.30 mA/mg_{Ag}, 109.80 mA/mg_{Ag}, 71.95 mA/mg_{Ag} (Figure 2d), respectively. Compared to the corresponding pure faceted-Ag_3PO_4 catalysts with carbon support, the mass-specific activity of the hybrid tetrahedron-Ag_3PO_4/cube-Cu_2O/C catalyst is 2.0 times that of pure tetrahedron-Ag_3PO_4/C catalyst, 6.4 times that of pure rhombic dodecahedron-Ag_3PO_4/C catalyst, and 6.5 times that of pure cube-Ag_3PO_4/C catalyst (Figure 2d). Obviously, hybrid rhombic dodecahedron-Ag_3PO_4/cube-Cu_2O/C catalysts possess the best electrochemical performance towards ORR among three hybrid different catalysts.

To further elucidate the relation between Ag_3PO_4 and Cu_2O, we conduct a variety of ORR electrocatalytic properties analyses. In our previous work, we have confirmed that rhombic dodecahedron-Ag_3PO_4 presents good electrochemically catalytic activity towards ORR under alkaline conditions.[22] Obviously, the cube-Cu_2O showed poor ORR performance (Figure S4), however, the ORR performance increased sharply when it was mixed with faceted-Ag_3PO_4. Briefly, the as-prepared rhombic dodecahedron-Ag_3PO_4/cube-Cu_2O/C (1: 0.125: 4) catalysts show a mass-specific activity of 109.80 mA/mg_{Ag}, which is 6.4 times that of a pure rhombic dodecahedron-Ag_3PO_4/C catalyst (17.20 mA/mg_{Ag}) (Figure 2). These data suggest that the Cu_2O does not participate in the ORR directly, and Ag_3PO_4 plays the role of an active component. These results support why there is an optimal mass ratio of Ag_3PO_4 and Cu_2O, to enhance the activity effectively, the usage of Cu_2O should be carefully added. It is worthwhile to point out that the poor ORR performance of mixture with too much Cu_2O could be attributed to poor electrochemical properties of Cu_2O. On the contrary, Cu_2O plays a limited role if the usage of Cu_2O is decreased.

To further identify the electronic interactions, XPS analysis of pure rhombic dodecahedron-Ag_3PO_4, pure cube-Cu_2O and the hybrid rhombic dodecahedron-Ag_3PO_4/cube-Cu_2O was carried out. Figure S6a presents the typical Ag 3d XPS spectra in the hybrid rhombic dodecahedron-Ag_3PO_4/cube-Cu_2O and pure rhombic dodecahedron-Ag_3PO_4. Compared to pure rhombic dodecahedron-Ag_3PO_4, the binding energy of Ag in the hybrid rhombic dodecahedron-Ag_3PO_4/cube-Cu_2O shifts positively. The oxidative state of Ag indicates that Ag in hybrid rhombic dodecahedron-Ag_3PO_4/cube-Cu_2O loses electrons in

© 2019 Wiley-VCH Verlag GmbH & Co. KGaA, Weinheim

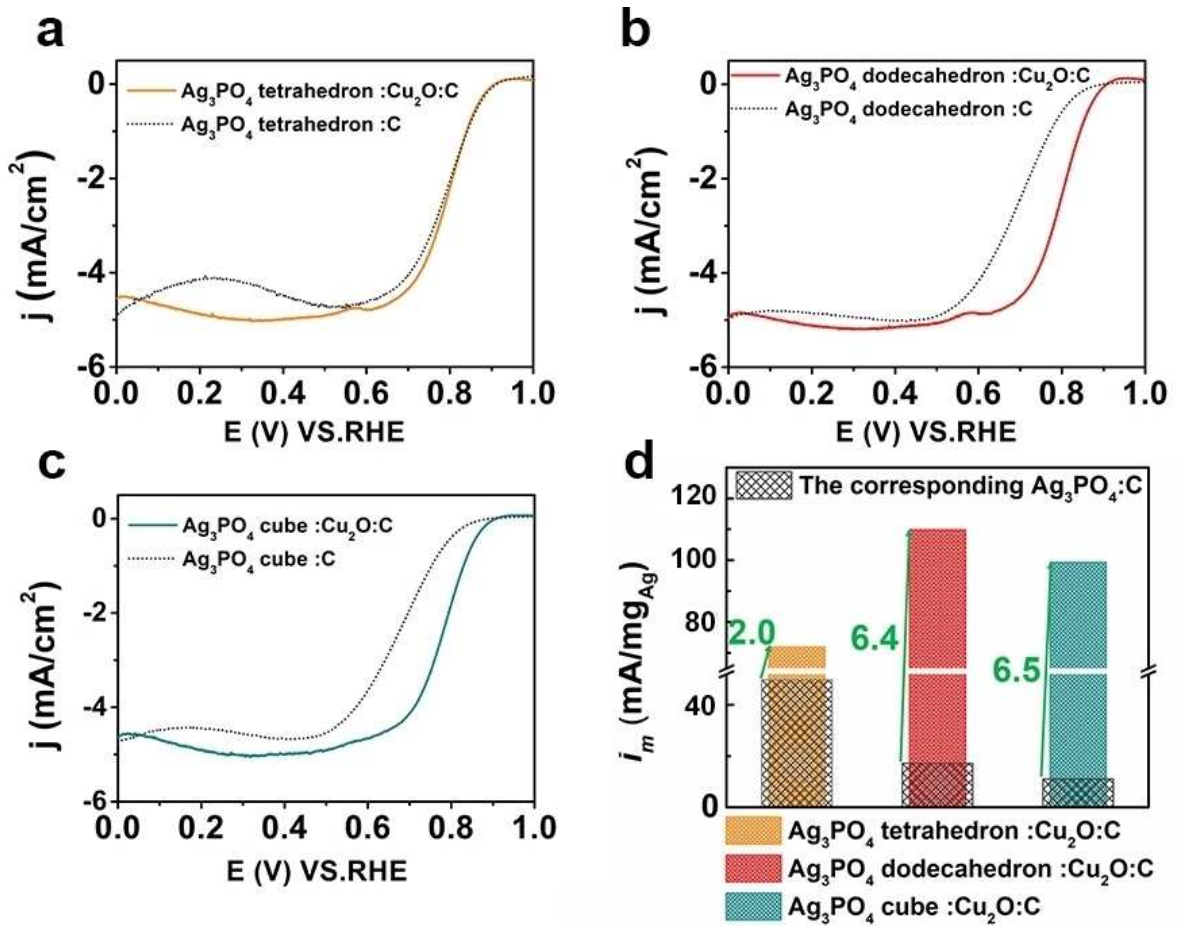

Figure 2. Comparison of electrocatalytic properties with the corresponding pure faceted-Ag_3PO_4: ORR polarization curves of hybrid (a) tetrahedron-; (b) rhombic dodecahedron-; (c) cube-Ag_3PO_4 and cube-Cu_2O supported on carbon catalysts in optimal proportions (1: 0.125: 4); (d) mass-specific activity of hybrid faceted-Ag_3PO_4 and cube-Cu_2O supported on carbon catalysts in optimal proportions (1: 0.125: 4).

the process of mixing with cube-Cu_2O. In addition, Figure S6b shows the typical Cu 2p XPS spectra in the hybrid rhombic dodecahedron-Ag_3PO_4/cube-Cu_2O and pure cube-Cu_2O. The negative shift of the Cu 2p3/2 peaks shows a more reduced state of Cu in hybrid rhombic dodecahedron-Ag_3PO_4/cube-Cu_2O, indicating that it has obtained more electrons. These results unambiguously demonstrate the electron donation from rhombic dodecahedron-Ag_3PO_4 to pure cube-Cu_2O.

Based on the experimental results, we proposed a mechanism for the enhanced ORR electrochemical activity of the different hybrid faceted-Ag_3PO_4/cube-Cu_2O catalyst. It has been reported that Ag_3PO_4 is an n-type semiconductor,[28] while Cu_2O has been reported as a p-type semiconductor.[29] On the basis of their respective Fermi level, a possible electron transfer behavior between these two semiconductors is drawn in Scheme 1 on the basis of energy band calculations.[30] According to the XPS analysis and semiconductor theory, the electrons transferred from Ag_3PO_4 to Cu_2O at the interface of these two semiconductors, leading to an electron-rich region for Cu_2O and an electron-deficient region for Ag_3PO_4. The DFT calculations on basis of the density of states (DOS) further reveal that the electron transfer (Figure 3f) from Ag_3PO_4 to Cu_2O effectively tunes the d-band structure of Ag in the hybrid Ag_3PO_4 and Cu_2O system, which results in upshifting ε_d of Ag in Ag_3PO_4 (110) surface from -2.32 to -2.26 eV (Figure 3c, e, and g). As clarified by d-band theory,[31,32] this upward shift in ε_d of Ag in the hybrid Ag_3PO_4/Cu_2O material will promote catalytic ORR reactions, since the upward shift of the Ag d-band will pull less of the antibonding states below the Fermi level, leading optimal adsorption of intermediates for Ag in the volcano plot of the oxygen binding energy and thus lead to higher ORR activities.[33]

To further support electron transfer theory proposed above, we mixed Ag_3PO_4 with another semiconductor TiO_2 as a comparison and recorded their ORR polarization curves and calculated mass-specific activity (Figure S5). Under the above-mentioned theory, the electron will transfer from TiO_2 to Ag_3PO_4 (Figure S7) according to energy band structure especially Fermi level of Ag_3PO_4 and TiO_2. The electron-rich region on the surface of Ag_3PO_4 will be no longer able to upshift ε_d of Ag (Figure 3a and g). Therefore, the adsorption energy of intermediates will become weaker and then the ORR mass-specific activity of hybrid $Ag_3PO_4/TiO_2/C$ catalyst compared with the pure Ag_3PO_4 catalyst will decrease. The experimental

© 2019 Wiley-VCH Verlag GmbH & Co. KGaA, Weinheim

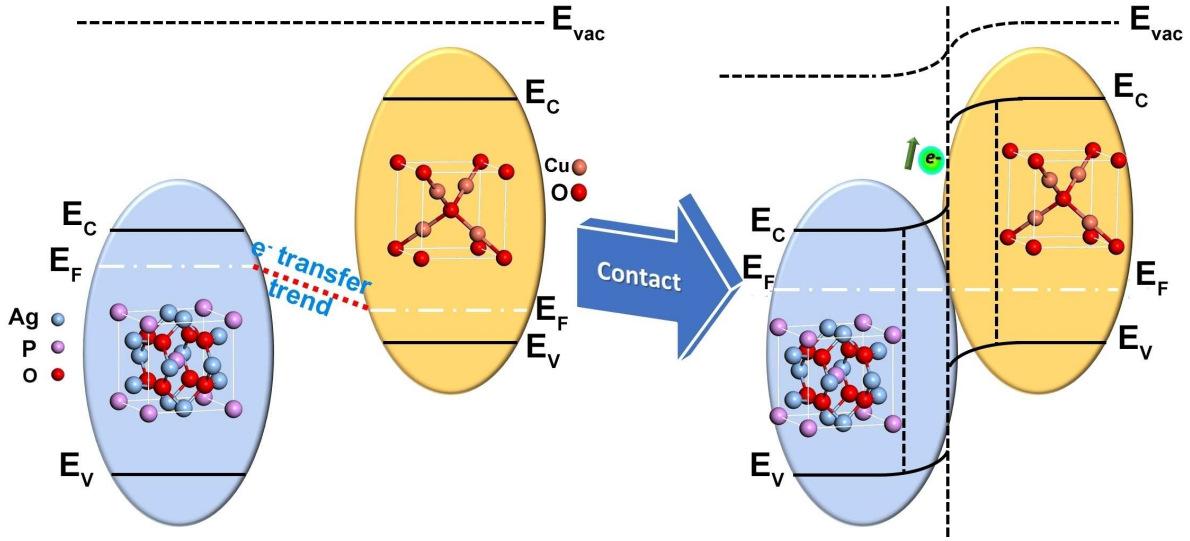

Scheme 1. Electron transfer behaviour at the interface of n-type semiconductor Ag_3PO_4 and p-type semiconductor Cu_2O.[a)a)] E_{vac}: Vacuum level, E_C: Conduction band, E_F: Fermi level, E_V: Valence band. For Ag_3PO_4, $E_C = -4.95$ eV, $E_V = -7.35$ eV and for Cu_2O, $E_C = -3.47$ eV, $E_V = -5.67$ eV.

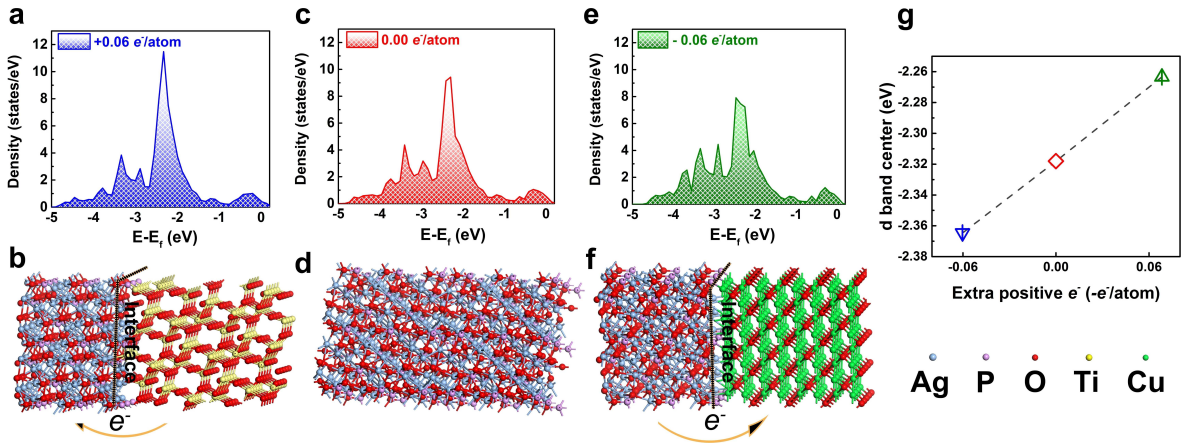

Figure 3. Projected d band density of Ag in Ag_3PO_4 under external charge with a density of (a) + 0.06, (c)0, (e)-0.06 eV/atom, the yellow vertical line indicates the corresponding d band center; the corresponding electron transfer schematic diagram at the interface of (b) Ag_3PO_4 and TiO_2, (d) pure Ag_3PO_4, (f) Ag_3PO_4 and Cu_2O; (g) dependence of the d band center of Ag in Ag_3PO_4 on extra charge.

results fell out as we had expected (Figure S5) that the ORR properties of Ag_3PO_4/TiO_2 compound decreased, which have strongly confirmed our theoretical analysis.

In summary, we have developed an electronically coupled Ag_3PO_4/Cu_2O hybrid electrocatalysts that present a huge improvement in electrocatalytic activity toward ORR as compared with corresponding pure Ag_3PO_4 catalysts. It provides a good way to achieve optimal adsorption of intermediates in the volcano plot of the oxygen binding energy and thus high ORR activities by tuning the d-band structure of Ag by utilizing the electron transfer at the interfacial junction of semiconductors. Our work paved a new way for the future efficient application of PEMFCs and exploited a new field in the rational design of non-Pt hybrid catalysts.

Supporting Information Summary

Experimental procedures, the density functional theory (DFT) calculation method, scanning electron microscope (SEM) images, X-ray diffraction pattern, electrocatalytic properties of various Ag_3PO_4 and Cu_2O, X-ray photoelectron spectroscopy (XPS) and schematic diagram of electron transfer are available in supporting information.

Acknowledgements

The work is sponsored by the thousand talents program for distinguished young scholars from Chinese government, National Key R&D Program of China (No. 2017YFB0406000), and National Natural Science Foundation of China (CN) (21875137, 51521004 and 51420105009), and start-up fund (JBW) and the Zhi-Yuan

© 2019 Wiley-VCH Verlag GmbH & Co. KGaA, Weinheim

Endowed fund (TD) from Shanghai Jiao Tong University. H. Z. thanks the financial support from the Shanghai Sailing Program (16YF1406000) and the computing resources from Shanghai Jiao Tong University Supercomputer Center.

Conflict of Interest

The authors declare no conflict of interest.

Keywords: Charge Separation Effect · Density Functional Theory · Fuel Cell · Oxygen Reduction Reaction · Semiconductor Heterojunction

[1] F. T. Wagner, B. Lakshmanan, M. F. Mathias, *J. Phys. Chem. Lett.* **2010**, *1*, 2204–2219.
[2] Z. Peng, H. Yang, *Nano Today* **2009**, *4*, 143–164.
[3] J. Wu, H. Yang, *Acc. Chem. Res.* **2013**, *46*, 1848–1857.
[4] M. K. Debe, *Nature* **2012**, *486*, 43–51.
[5] H. A. Gasteiger, S. S. Kocha, B. Sompalli, F. T. Wagner, *Appl. Catal., B* **2005**, *56*, 9–35.
[6] L. Zhang, L. T. Roling, X. Wang, M. Vara, M. Chi, J. Liu, S.-I. Choi, J. Park, J. A. Herron, Z. Xie, *Science* **2015**, *349*, 412–416.
[7] L. Bu, N. Zhang, S. Guo, X. Zhang, J. Li, J. Yao, T. Wu, G. Lu, J. Y. Ma, D. Su, *Science* **2016**, *354*, 1410–1414.
[8] C. Chen, Y. Kang, Z. Huo, Z. Zhu, W. Huang, H. L. Xin, J. D. Snyder, D. Li, J. A. Herron, M. Mavrikakis, *Science* **2014**, *343*, 1339–1343.
[9] D. Wang, H. L. Xin, R. Hovden, H. Wang, Y. Yu, D. A. Muller, F. J. DiSalvo, H. D. Abruña, *Nat. Mater.* **2013**, *12*, 81–87.
[10] T. Bian, H. Zhang, Y. Jiang, C. Jin, J. Wu, H. Yang, D. Yang, *Nano Lett.* **2015**, *15*, 7808–7815.
[11] J. Wu, J. Zhang, Z. Peng, S. Yang, F. T. Wagner, H. Yang, *J. Am. Chem. Soc.* **2010**, *132*, 4984–4985.
[12] J. Wu, A. Gross, H. Yang, *Nano lett.* **2011**, *11*, 798–802.
[13] J. Wu, L. Qi, H. You, A. Gross, J. Li, H. Yang, *J. Am. Chem. Soc.* **2012**, *134*, 11880–11883.
[14] V. Mazumder, Y. Lee, S. Sun, *Adv. Funct. Mater.* **2010**, *20*, 1224–1231.
[15] R. Bashyam, P. Zelenay, *Nature* **2006**, *443*, 63–66.
[16] E. Antolini, *Energy Environ. Sci.* **2009**, *2*, 915–931.
[17] L. Xiao, L. Zhuang, Y. Liu, J. Lu, *J. Am. Chem. Soc.* **2008**, *131*, 602–608.
[18] B. Blizanac, P. N. Ross, N. Marković, *J. Phys. Chem. B* **2006**, *110*, 4735–4741.
[19] M. Lefèvre, E. Proietti, F. Jaouen, J.-P. Dodelet, *Science* **2009**, *324*, 71–74.
[20] Y. Y. Liang, Y. G. Li, H. L. Wang, J. G. Zhou, J. Wang, T. Regier, H. J. Dai, *Nat. Mater.* **2011**, *10*, 780–786.
[21] J. Suntivich, H. A. Gasteiger, N. Yabuuchi, H. Nakanishi, J. B. Goodenough, Y. Shao-Horn, *Nat. Chem.* **2011**, *3*, 546–550.
[22] Y. Qin, F. Li, P. Tu, Y. Ma, W. Chen, F. Shi, Q. Xiang, H. Shan, L. Zhang, P. Tao, C. Song, W. Shang, T. Deng, H. Zhu, J. Wu, *RSC Adv.* **2018**, *8*, 5382–5387.
[23] C. Li, P. Zhang, R. Lv, J. Lu, T. Wang, S. Wang, H. Wang, J. Gong, *Small* **2013**, *9*, 3951–3956.
[24] Y. Hou, F. Zuo, Q. Ma, C. Wang, L. Bartels, P. Feng, *J. Phys. Chem. C* **2012**, *11*, 20132–20139.
[25] Z. Li, K. Dai, J. Zhang, C. Liang, G. Zhu, *Mater. Lett.* **2017**, *206*, 48–51.
[26] S. B. Rawal, S. Do Sung, W. I. Lee, *Catal. Commun.* **2012**, *17*, 131–135.
[27] W. C. Huang, L. M. Lyu, Y. C. Yang, M. H. Huang, *J. Am. Chem. Soc.* **2012**, *134*, 1261–1267.
[28] Z. J. Yi, J. H. Ye, N. Kikugawa, T. Kako, S. X. Ouyang, H. Stuart-Williams, H. Yang, J. Y. Cao, W. J. Luo, Z. S. Li, Y. Liu, R. L. Withers, *Nat. Mater.* **2010**, *9*, 559–564.
[29] H. Raebiger, S. Lany, A. Zunger, *Phys Rev B* **2007**, *76*, 045209.
[30] J. T. Li, N. Q. Wu, *Catal. Sci. Technol.* **2015**, *5*, 1360–1384.
[31] M. Mavrikakis, B. Hammer, J. K. Nørskov, *Phys. Rev. Lett.* **1998**, *81*, 2819–2822.
[32] J. Greeley, J. K. Nørskov, M. Mavrikakis, *Annu. Rev. Phys. Chem.* **2002**, *53*, 319–348.
[33] J. K. Norskov, J. Rossmeisl, A. Logadottir, L. Lindqvist, J. R. Kitchin, T. Bligaard, H. Jonsson, *J. Phys. Chem. B* **2004**, *108*, 17886–17892.

Submitted: February 16, 2019
Accepted: April 25, 2019

© 2019 Wiley-VCH Verlag GmbH & Co. KGaA, Weinheim